2*p* resonant photoemission study of TiO_2

K. C. Prince and V. R. Dhanak
Sincrotrone Trieste S.c.p.A., Padriciano 99, Trieste, Italy

P. Finetti, J. F. Walsh, R. Davis, C. A. Muryn, H. S. Dhariwal, and G. Thornton
Department of Chemistry, University of Manchester, Manchester, United Kingdom

G. van der Laan
SRS, Daresbury Laboratory, Warrington WA4 4AD, United Kingdom
(Received 12 June 1996; revised manuscript received 5 November 1996)

Resonant photoemission measurements of $TiO_2(100)$ at the Ti $L_{2,3}$ edge are reported. For transitions from $2p$ to $3d$ states of e_g symmetry there is a resonance enhancement of the intensity of the band-gap defect states by a factor of 6. The valence band shows resonance enhancements for transitions to states of both e_g and t_{2g} symmetry. The maximum enhancement of 3 for the high binding energy indicates that the whole of the O $2p$ derived valence band is hybridized with Ti $3d$ states, with the higher binding-energy part being more strongly mixed. The defect-state resonances are broader than the absorption resonances and have a width of about 4 eV due to the multiplet structure. [S0163-1829(97)00912-0]

I. INTRODUCTION

Tjeng *et al.*[1] have reported the L_3 x-ray-absorption spectrum of CuO and photoemission spectra at photon energies near the absorption maximum. Giant resonance effects were observed and important information relating to the ground-state electronic configuration of the oxide was extracted. This work stimulated us to investigate an oxide at the other end of the $3d$ series of elements, TiO_2, and to measure resonant photoemission spectra (RESPES) at the corresponding $L_{2,3}$ edges.

As discussed by Okada and Kotani[2] and Tanaka and Jo[3] for the cases of photoemission and photoabsorption, the main configurations in the Anderson impurity model for the ground state of TiO_2 can be described as a mixture of $3d^0$, $3d^1\underline{L}$, and $3d^2\underline{LL}$ states, where $\underline{L}$ denotes a hole of appropriate symmetry on the adjacent oxygen (ligand) site. These configurations have relative energy positions of 0, Δ, and $2\Delta+U$, respectively, where Δ is the charge-transfer energy required to remove an electron from an oxygen state and place it into a d state, and U is the on-site $3d$-$3d$ Coulomb repulsion. Okada and Kotani[2] have explained the observed Ti $L_{2,3}$ or $2p$ x-ray absorption spectra (XAS) and x-ray photoelectron spectra (XPS) of TiO_2 using the following parameters:

$$\Delta(e_g)=4, \quad U=4, \quad Q=6 \text{ eV},$$

$$V(e_g)=-2V(t_{2g})=6 \text{ eV},$$

$$\Delta(e_g)-\Delta(t_{2g})=10Dq=1.7 \text{ eV},$$

where Q is the $2p-3d$ Coulomb repulsion, $10Dq$ is the crystal-field interaction parameter, which splits the e_g and t_{2g} states, and $V(t_{2g})$ and $V(e_g)$ are the strength of Ti $3d$ $-$O $2p$ hybridization. This results in weights of 39.5% d^0, 48.2% d^1, and 12.3% d^2 for the ground state, giving an average charge on the Ti atom of 0.73 electrons. Although the rutile structure has symmetry D_{2h}, it is only slightly perturbed from O_h and so the irreducible representations of this group will be used.

Resonant photoemission may occur for a transition from a ground state to a final state via two interfering channels. Direct photoemission from the valence state $3d^n$ gives a final state: $3d^{n-1}+e$. This state can also be reached via x-ray absorption to a $2p^5 3d^{n+1}$ state followed by a $2p3d3d$ decay (Table I), so interference effects and resonant enhancement may occur.

Previous RESPES studies of titanium oxides have been carried out at the $M_{2,3}$ or $3p$, edge of Ti.[4–10] At this edge, the primarily oxygen $2p$ derived valence band is found to display a broad resonance (10–15 eV wide) at an energy somewhat above the optical threshold for $3p$ emission. The strength of the resonant effects varies across the valence band, being stronger at higher binding energy, which was interpreted as indicating that the states have more bonding character. The strength of the resonance has been correlated with the extent of hybridization of Ti d character states with the oxygen ligand or valence states of p character. Courths, Cord, and Saalfeld[7] hypothesized that the enhancement of the low-binding-energy valence states indicated Ti $4sp$ hybridization.

TABLE I. Configuration in the ground state, XAS state, and photoemission final states of TiO_2. The configuration mixing is indicated by double sided arrows. e indicates a photoemitted electron in the continuum.

Ground state	$3d^0$	$\leftrightarrow$	$3d^1\underline{L}$	$\leftrightarrow$	$3d^2\underline{LL}$
Dipole transition	$\downarrow$		$\downarrow$		$\downarrow$
XAS state	$\underline{2p}3d^1$	$\leftrightarrow$	$\underline{2p}3d^2\underline{L}$	$\leftrightarrow$	$\underline{2p}3d^3\underline{LL}$
autoionization			$\downarrow$		$\downarrow$
XPS valence state			$3d^0\underline{L}+e$	$\leftrightarrow$	$3d^1\underline{LL}+e$

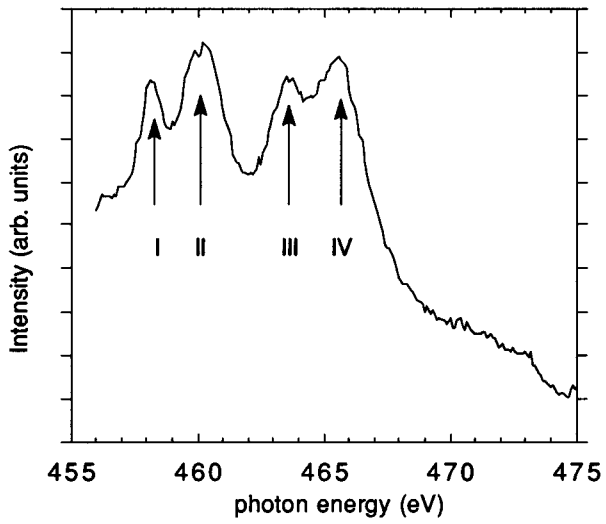

FIG. 1. $L_{2,3}$ NEXAFS spectrum of TiO_2.

II. EXPERIMENT

The measurements were carried out on beamlines U5.1 and 1.1 at the Daresbury SRS; the former is a 10 period undulator with a plane grating monochromator, while the latter is a bending magnet beamline with a spherical grating monochromator. Higher-order radiation was not a problem for the measurements on line U5.1, but second-order radiation presented some difficulties for the data taken at line 1.1. The second-order light excited the Ti 2*p* levels giving spurious structures overlapping the valence band. These structures were easily recognized as, on changing the photon energy, they moved by twice the energy increment. During data processing, these peaks were subtracted from the spectra by fitting the peak shape and intensity at photon energies where the peak appeared above the Fermi level. This fitted peak was displaced by twice the photon energy increment between spectra and then subtracted.

For the experiments on U5.1, the $TiO_2(100)$ crystal was prepared by sputtering, and annealing in oxygen for 5 min at 2×10^{-6} mbar and 850 K. The sample was then cooled in oxygen to 600 K before pumping away the oxygen. This treatment reduces the number of oxygen vacancy defects but does not eliminate them entirely. For the experiments on line 1.1 the sample was prepared by sputtering and annealing only, which increases the number of defects.

The analyzer used was a VSW Scientific Instruments 100-mm mean radius hemispherical electron energy analyzer with a 16 channel detector. XAS were measured using the Auger yield. Photon energies were calibrated to the values given by van der Laan,[11] and all spectra were taken in normal emission with an angle of incidence of the light equal to 40°. The sample was at room temperature and the spectra were normalized to the photon flux using a copper grid. The Fermi level was determined by emission from the tantalum supports.

III. RESULTS AND DISCUSSION

Figure 1 shows the Ti $L_{2,3}$ near-edge x-ray-absorption spectrum. It is similar to that of van der Laan,[11] although we reduced our resolution to obtain a higher intensity which is

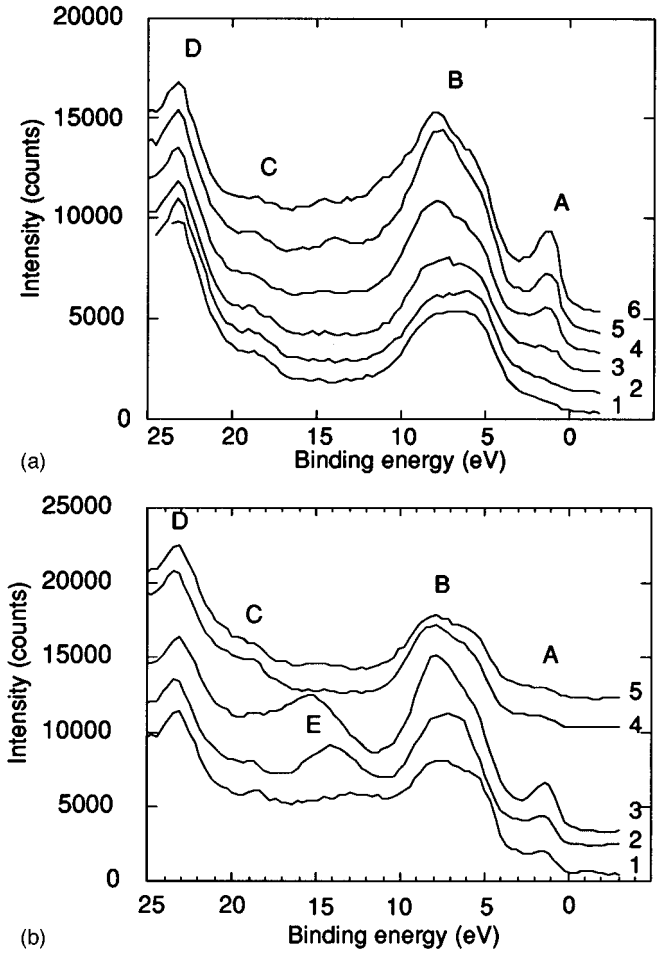

FIG. 2. (a) Normal-emission photoelectron spectra of the valence band of TiO_2 at the following energies: (1) 454 eV; (2) 455 eV; (3) 458.6 eV; (4) 459.2 eV; (5) 460.2 eV. (b) Same as (a) except with the following photon energies: (1) 462.4 eV; (2) 464.2 eV; (3) 465.9 eV; (4) 470 eV; (5) 472 eV.

necessary for photoemission. Van der Laan has identified the peaks I to IV as being due to transitions to the following final states:

$$\begin{aligned} &\text{I} \quad \underline{2p_{3/2}}3d(t_{2g}),\\ &\text{II} \quad \underline{2p_{3/2}}3d(e_g),\\ &\text{III} \quad \underline{2p_{1/2}}3d(t_{2g}),\\ &\text{IV} \quad \underline{2p_{1/2}}3d(e_g). \end{aligned}$$

As above, underlining represents a hole state. This spectrum arises because of the spin-orbit splitting of the core hole, which is 5.7 eV, and the splitting of the final *d* states by crystal-field interaction. For octahedral symmetry, peaks I and II (III and IV) are split into e_g and t_{2g} peaks separated by an energy $10Dq$, which as noted above has a value of 1.7 eV. The e_g state has the higher energy because the associated *d* orbitals are directed towards the oxygen atoms. When the symmetry is distorted from O_h, as in the rutile structure, the e_g peak is broadened.[12] At 13-eV photon energy above the main peak, there are weaker satellites which have not been studied here.

Figure 2(a) and 2(b) shows a series of photoemission spectra taken at selected photon energies. The valence band *B* shows a substantial variation in intensity with a maximum change of about a factor 3. In addition, the defect states *A*

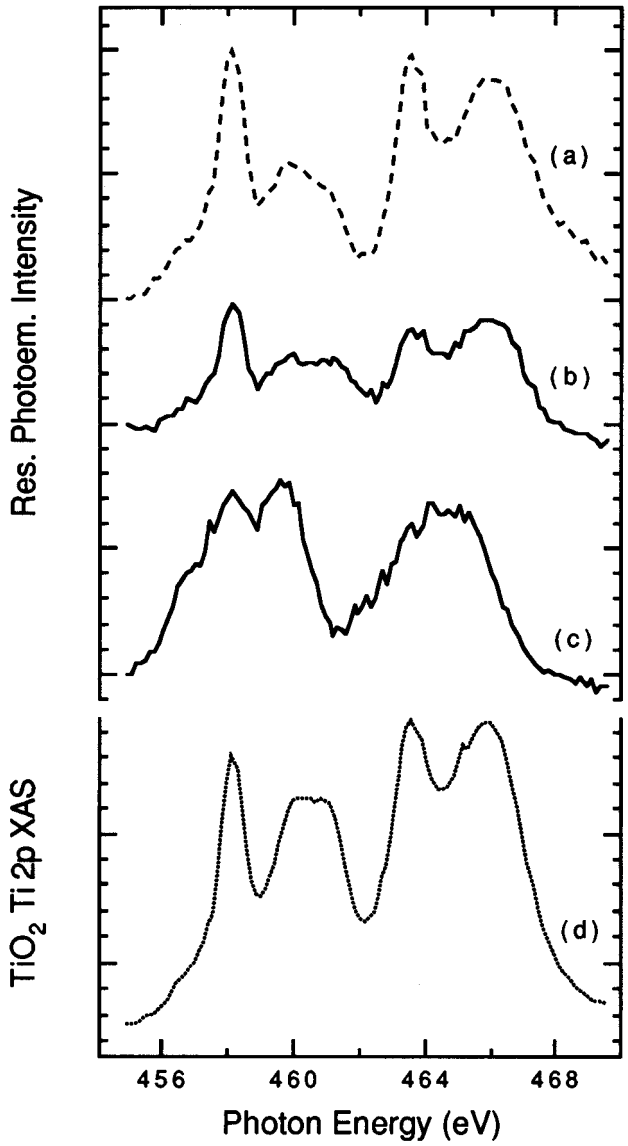

FIG. 3. Resonant photoemission intensity of the valence band and defect states at binding energies of (a) 8.2 eV (dashed line); (b) 4.6 eV (full line); (c) defect states (full line); (d) absorption spectrum (dotted line).

above the valence band show a resonant enhancement of about a factor of 6 in intensity. Features E shifts and appears to have constant kinetic energy; it is therefore assigned to an Auger peak. The peak C is assigned to final states $3d^1\underline{L}^2$, i.e., with two ligand holes. Because of its weakness, it was not possible to study this peak in more detail, but it also appears to show some resonance behavior. Other satellites expected at 12 and 15 eV were not resolved. The peak D is assigned to emission from the oxygen 2s level.

Constant initial state (CIS) spectra of the valence and defect states, are plotted in Fig. 3 together with the absorption curve. The CIS curves were generated by eliminating the second-order contribution and then adding the intensities at the following binding energies: defect peak: 1.8–2.4 eV; low-binding-energy states: 4.3–4.9 eV; high-binding-energy states: 7.8–8.5 eV. The CIS spectrum of the high-binding-energy states shown in Fig. 3(a), contains strong maxima in the RESPES intensity at photon energies corresponding to peaks I–IV in the XAS curve. The resonances follow the absorption curve closely and the widths of the resonances are equal to the widths of the x-ray-absorption peaks. The low-binding-energy states also resonant but less strongly.

The behavior of the defect states, whose CIS spectrum is shown in Fig. 3(c), is rather different. Two broad resonances are observed centered roughly around the average energy of peaks I and II, and III and IV, respectively. This resonance curve is expected to have a different spectral form since at the oxygen vacancy site at least, an oxygen ligand is missing. The symmetry is thus broken and the ground-state spectrum is dominated by the Ti d^1 state. Given that the bonding part of the valence-band follows the absorption curve closely, we may surmise that the defect state resonance curve also reflects the local density of states. Thus RESPES provides us with a means of obtaining the XAS curve projected on the defect site which is difficult to obtain otherwise. In general, the spectrum will not be quantitatively equal to a near-edge x-ray-absorption fine-structure (NEXAFS) spectrum because the RESPES is modulated by an Auger matrix element rather than a dipole matrix element. However, the good agreement between the spectral form of the valence-band NEXAFS and RESPES is encouraging.

Since the defect site initial state is dominated by Ti d^1 states, it is reasonable to expect that the NEXAFS spectrum will be similar to that of Ti_2O_3. The NEXAFS spectrum of Park[13] is indeed rather similar to the RESPES spectrum reported here. This provides further evidence that RESPES can give the site selective NEXAFS spectrum to a good approximation.

The conditions under which this approximation is valid depend on the Fano[14] parameter q. If q has a low value, the RESPES may be considerably broadened and shifted. It has been estimated that a necessary condition for the NEXAFS and RESPES spectra to be similar is $q>10$.[15]

The width of these peaks is 4 eV, too large to be due to the x-ray-absorption final-state lifetime broadening, or heterogeneity. We assign the main part of this broadening to multiplet splitting on the basis of the calculations of van der Laan and Kirkman.[12] These calculations were carried out for d^0 and d^1 Ti atoms in octahedral and tetrahedral symmetry, but should apply as well to the present case of defects in a low symmetry environment. The d^0 initial state displays four peaks, but the d^1 initial state displays a richer structure due to multiplet splitting. The relative intensities of the peaks depends on the strength of the crystal-field splitting.

The most direct information extracted from previous RESPES data for Ti oxides has been the extent of hybridization of the Ti d states with the mainly oxygen derived p states. From the present results we are able to say that primarily the bonding part of the valence band is hybridized more strongly with Ti states because this part of the valence-band emission resonates more strongly. Older tight-binding calculations[16] indicated Ti d hybridization across the band, but more recent calculations[17] indicate that the orbital mixing is stronger in the higher-binding-energy part. The present results support these calculations, and confirm the conclusion of Heise, Courths, and Witzel[9] based on the $M_{2,3}$ RESPES.

Notable differences between the present results and pre-

vious photoemission studies[4–9] at the $M_{2,3}$ edges are first that there is no delayed onset as the effects occur at the thresholds, and second the narrow energy range of the effects. Since the effects that we observe are clearly linked to strong $2p \rightarrow 3d$ absorption, they are more easily interpreted. In the case of $M_{2,3}$ absorption, there is the possibility that $3p \rightarrow 4s$ transitions are also involved, and that the resonance indicates which parts of the valence band are hybridized with Ti s states. This indeed appears to have been the case, as suggested by Heise, Courths, and Witzel.[9] The $M_{2,3}$ resonance appears to involve XAS states which are not pure Ti $3d$, but contain considerable $4sp$ character: thus both the $3d$ and $4sp$ hybridized oxygen states resonate. Only the present $L_{2,3}$ spectra can confirm this interpretation of the $M_{2,3}$ data.

The effects seen here are comparable in magnitude with the resonant enhancement of the valence band of CuO for a d^8 final state (about a factor of 6), but much weaker than the giant enhancement of the $d^9\underline{L}$ satellite (two orders of magnitude.) Tanaka and Jo[3] predicted enhancements that are much larger than those observed here, but they calculated the effect on the Ti d states only. As the d and O $2p$ states overlap, we cannot say how large the enhancement of the pure d component is.

IV. SUMMARY

Resonant valence-band photoemission spectra in the vicinity of the Ti $L_{2,3}$ edge have been reported. Both the bonding part of the valence band of TiO_2 and vacancy induced defect states show increases in intensity for photon energies corresponding to L_2 and L_3 absorption maxima. Since the magnitude of the effect is comparable to that observed for CuO, a late transition-metal oxide, this confirms that metal-oxygen hybridization is also strong for early $3d$ metal oxides, supporting the conclusion of Okada and Kotani.[2] We suggest that to a good approximation, resonant photoemission gives a NEXAFS-like spectrum of the density of states.

ACKNOWLEDGMENT

This work was supported by the British Council under Project No. ROM/889/92/87.

[1] T. H. Tjeng, C. T. Chen, J. Ghijsen, P. Rudolf, and F. Sette, Phys. Rev. Lett. **67**, 501 (1991).
[2] K. Okada and A. Kotani, J. Electron Spectrosc. Relat. Phenom. **62**, 131 (1993).
[3] A. Tanaka and T. Jo, J. Phys. Soc. Jpn. **63**, 2788 (1994).
[4] R. L. Kurtz, R. Stockbauer, T. E. Madey, E. Roman, and J. L. de Segovia, Surf. Sci. **218**, 178 (1989).
[5] E. Bertel, R. Stockbauer, and T. E. Madey, Phys. Rev. B **27**, 1939 (1983).
[6] K. E. Smith and V. E. Henrich, Solid State Commun. **68**, 29 (1988).
[7] R. Courths, B. Cord, and H. Saalfeld, Solid State Commun. **70**, 1047 (1989).
[8] Z. Zhang, S.-P. Jeng, and V. E. Henrich, Phys. Rev. B **43**, 12 004 (1991).
[9] R. Heise, R. Courths, and S. Witzel, Solid State Commun. **84**, 599 (1992).
[10] S. Shin, Y. Tezuka, T. Ishii, and Y. Ueda, Solid State Commun. **87**, 1051 (1993).
[11] G. van der Laan, Phys. Rev. B **41**, 12 366 (1990).
[12] G. van der Laan and I. W. Kirkman, J. Phys. Condens. Matter **4**, 4189 (1992).
[13] J. Park, Ph.D. thesis, University of Michigan, 1994.
[14] U. Fano, Phys. Rev. **124**, 1866 (1961).
[15] G. van der Laan, B. T. Thole, H. Ogasawara, Y. Seino, and A. Kotani, Phys. Rev. B **46**, 7221 (1992).
[16] M. Munnix and M. Schmeits, Phys. Rev. B **30**, 2202 (1984).
[17] F. M. F. de Groot, J. Faber, J. J. M. Michiels, M. T. Czyzyk, M. Abbate, and J. Fuggle, Phys. Rev. B **48**, 2074 (1993).